We are IntechOpen, the world's leading publisher of Open Access books Built by scientists, for scientists

4,800
Open access books available

122,000
International authors and editors

135M
Downloads

Our authors are among the

154
Countries delivered to

TOP 1%
most cited scientists

12.2%
Contributors from top 500 universities

CLARIVATE ANALYTICS BOOK CITATION INDEX INDEXED

WEB OF SCIENCE™

Selection of our books indexed in the Book Citation Index in Web of Science™ Core Collection (BKCI)

Interested in publishing with us?
Contact book.department@intechopen.com

Numbers displayed above are based on latest data collected.
For more information visit www.intechopen.com

5

Flexible Micro Gas Turbine Rig for Tests on Advanced Energy Systems

Mario L. Ferrari and Matteo Pascenti
University of Genoa – Thermochemical Power Group (TPG)
Italy

1. Introduction

During the last 15-20 years, microturbine (mGT) technology has become particularly attractive for power generation, especially in the perspective of the development of a distributed generation market (Kolanowski, 2004). The main advantages related to microturbines, in comparison to Diesel engines, are:

- smaller size and weight;
- fuel flexibility;
- lower emissions;
- lower noise;
- vibration-free operation;
- reduced maintenance.

The development of a laboratory based on a large size gas turbine is usually not feasible at the University level for high costs of components and plant management. However, the microturbine (mGT) technology (Kolanowski, 2004) allows wide-ranging experimental activities on small size gas turbine cycles with a strong cost reduction.

Moreover, this technology is promising from co-generative (and tri-generative) application point of view (Boyce, 2010), and is essential for advanced power plants, such as hybrid systems (Massardo et al., 2002), humid cycles (Lindquist et al., 2002), or externally fired cycles (Traverso et al., 2006).

However, if microturbine standard cycle is modified by introducing innovative components, such as fuel cells (Magistri et al., 2002, 2005), saturators (Pedemonte et al., 2007) or new concept heat exchangers (such as ceramic recuperators (McDonald, 2003)), at least two main aspects have to be considered:

- avoiding dangerous conditions (e.g.: machine overspeed, surge, thermal and mechanical stress, carbon deposition);
- ensuring the proper feeding conditions to both standard and additional components.

Moreover, the operation with new devices generates additional variables to be monitored, new risky conditions to be avoided and requires additional control system facilities (Ferrari, 2011).

Experimental support is mandatory to develop advanced power plants based on microturbine technology and to build reliable systems ready for commercial distribution. A possible cheap solution to perform laboratory tests is related to emulator facilities able to generate similar effects of a real system. These are experimental rigs designed to study

various critical aspects of advanced power plants without the most expensive components (e.g. fuel cells, high temperature heat exchangers). An important experimental study with mGT based emulators is running at U.S. DOE-NETL laboratories of Morgantown (WV-USA). This activity is based on a test rig designed to emulate cathode side of hybrid systems based on Solid Oxide Fuel Cell (SOFC) technology (Tucker et al., 2009). It is mainly composed of a recuperated microturbine, a fuel cell vessel (without ceramic material), an off-gas burner vessel, and a combustor controlled by a fuel cell real-time model (Tucker et al., 2009). Another emulator facility equipped with a micro gas turbine is under development at German Aerospace Center (DLR), Institute of Combustion Technology, of Stuttgard (Germany) (Hohloch et al., 2008). Its general layout is similar to the NETL test rig. However, this experimental plant includes a fuel cell vessel able to emulate the real stack exhaust gas composition with a water cooling system (coupled with an additional combustor) (Hohloch et al., 2008).

At University of Genoa, TPG researchers developed a new test rig based on a commercial recuperated 100 kW micro gas turbine equipped with a set of additional pipes and valves for flow management. These pipes are essential to perform high fidelity mass flow rate measurements and to connect the machine to an external modular vessel. This additional volume is located between the recuperator outlet (cold side) and the combustor inlet (Ferrari et al., 2009a) to emulate the dimensions of advanced cycle components (such as fuel cells (Ferrari et al., 2009a; Tucker et al., 2009), externally fired gas turbine facilities (Traverso et al., 2006), saturators (Pedemonte et al., 2007)).

This test rig, developed to carry out experimental tests in both steady-state and transient conditions, is designed to have the highest plant flexibility performance. In details, this facility is able to operate in the following configurations:

- simple cycle;
- recuperated and partly recuperated cycle;
- both simple and recuperated cycles coupled with a modular vessel for the emulation of additional component volume (Ferrari et al., 2009a);
- emulation of hybrid systems (Ferrari et al., 2010a) with high temperature fuel cell stack (cathodic and anodic vessels, anodic recirculation (Ferrari et al., 2010a), steam injection for chemical composition emulation, real-time model for components not present in the rig);
- co-generative and tri-generative (with an absorber cooler) systems.

Moreover, on all these plant layouts it is possible to test the influence of the following properties, especially in transient conditions:

- ambient temperature;
- volume size (downstream of the compressor);
- valve fractional opening values;
- bleed mass flow rates;
- grid connection or stand-alone systems;
- control system.

This chapter shows some examples of tests carried out with the rig (using different plant layouts and operative conditions), inside different research projects and during educational activities. In details, the facility was mainly developed inside two Integrated Projects of the EU VI Framework Program (Felicitas and Large-SOFC) and now it is involved in the new EU VII Framework (E-HUB Project) for tests to be carried out with an absorption cooler (tri-

generative configuration). Moreover, this experimental plant is essential to introduce undergraduate students to micro gas turbine technology, and Ph.D.s to advanced experimental activities in the same field. With this experimental rig, in addition to learning about thermodynamic cycles and plant layouts, students can also become familiar with their materials, piping, gaskets, technology for auxiliaries, and instrumentation.

2. Nomenclature

CAD	Computer Aided Design
CC	Combustion Chamber
CFD	Computational Fluid Dynamic
Ex	heat Exchanger
FC	Fuel Cell
GT	Gas Turbine
HS	Hybrid System
ISO	International Organization for Standardization
LAN	Local Area Network
mGT	micro Gas Turbine
mHAT	micro HAT cycle
NETL	National Energy Technology Laboratory
REC	RECuperator
RRFCS	Rolls-Royce Fuel Cell Systems
SOFC	Solid Oxide Fuel Cell
UDP	User Datagram Protocol
WHEx	Water Heat Exchanger
Variables	
COP	Coefficient Of Performance
h	heat transfer convective coefficient [W/m^{2}K]
I	current density [A/m^2]
i, j	indexes for Fig. 18
K_p	surge margin
m	mass flow rate [kg/s]
N	rotational speed [rpm]
n	number of moles
p	pressure [Pa]
P	power [W]
q	heat flux [W]
S	surface [m^2]
T	temperature [K]
TIT	Turbine Inlet Temperature [K]
TOT	Turbine Outlet Temperature [K]
U_f	fuel utilization factor
Greek symbols	
β	compressor pressure ratio (total to static)
Δ	variation
ε	recuperator effectiveness
λ	conductivity [W/mK]

Subscripts

0, 1, 2, 3, 4, 5, i	subscripts for Fig. 18
amb	ambient
c	compressor
d	on design
in	inlet
M	measured
s.l.	surge line
t	total

3. The commercial machine

The basic machine is a Turbec T100 PHS Series 3 (Turbec, 2002). It is equipped to operate in stand-alone configuration or connected to the electrical grid. This commercial unit consists of a power generation module (100 kW at nominal conditions), a heat exchanger located downstream of the recuperator outlet (hot side) for co-generative applications, and two battery packages for the start-up phase in stand-alone configuration. Even if the machine is located indoors, the outdoor roof was placed over the machine to use its air pre-filters. Figure 1 shows the plant layout diagram of the micro gas turbine as furnished by the manufacturer in the PHS configuration.

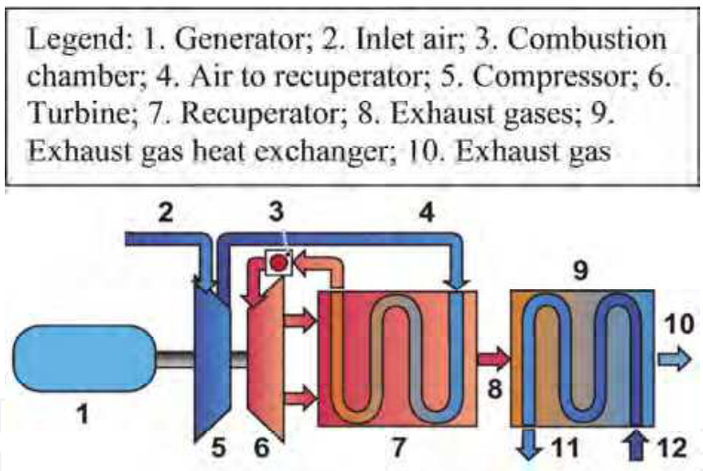

Fig. 1. Turbec T100 machine: PHS standard layout (courtesy of Turbec).

The power module (Fig. 2) is composed of a single shaft radial machine (compressor, turbine, synchronous generator) operating at a nominal rotational speed of 70000 rpm and a TIT of 950°C (1223.15 K), a natural gas fed combustor, a primary-surface recuperator, a power electronic unit (rectifier, converter, filters and breakers), an automatic control system interfaced with the machine control panel, and the auxiliaries. In this test rig the micro gas turbine is operated using its commercial control system. It works at constant rotational speed when the machine is in stand-alone mode. In this mode the control system changes the fuel mass flow rate to maintain the shaft (in steady-state condition) at 67550 rpm. In grid-connected mode this controller works at constant turbine outlet temperature (TOT). So, in this second mode the control system changes the fuel mass flow rate to maintain the

machine TOT (in steady-state condition) at 645°C (918.15 K). However, in both modes the power electronic system allows to generate a 50 Hz current output (at each load values).

Fig. 2. The T100 power module installed at the laboratory of the University of Genoa (power electronics and control system are not shown).

The heat exchanger for water heating (for cogenerative and trigenerative applications) includes an exhaust gas bypass device to control water temperature values. Each start-up battery package includes thirty 12 Volt batteries connected in series for a nominal voltage of 360 Volt DC.
The machine, in its commercial configuration, is equipped with the following essential probes for control reasons: electrical power (±1%), rotational speed (±10 rpm), TOT (±1.5 K), fractional opening values (pilot and main fuel valves), intake temperature, and heating water temperature meters. Furthermore, the commercial machine is equipped with diagnostic probes (e.g. vibration sensor, filter differential pressure meter, temperature probes for the auxiliary systems).
The TPG laboratory was also equipped with a 100 kW resistor bank (pure resistive load) for turbine operation in stand-alone mode. The bank is cooled through an air fan and continuously controlled by an inverter.

4. Machine modifications and connection pipes

The commercial power unit was modified for coupling with the external connection pipes used for flow measurement and management purposes. These modifications are essential

for measuring all the properties necessary for cycle characterization (e.g. air mass flow rate or recuperator boundary temperatures), not available in the commercial layout of the machine. For this reason the following modifications were carried out:

- the two pipes between the recuperator and the combustor inlet were substituted with four pipes for the external connections (Fig. 3);
- at the compressor outlet a check valve (Fig. 3) was introduced to prevent damage and block compressor backflow if surge conditions occur during experimental tests;
- between this valve and the recuperator inlet a T-joint was introduced to have a recuperator bypass line which is necessary for studying non-recuperated cycles or hybrid system start-up and shutdown phases (Ferrari et al., 2010a).

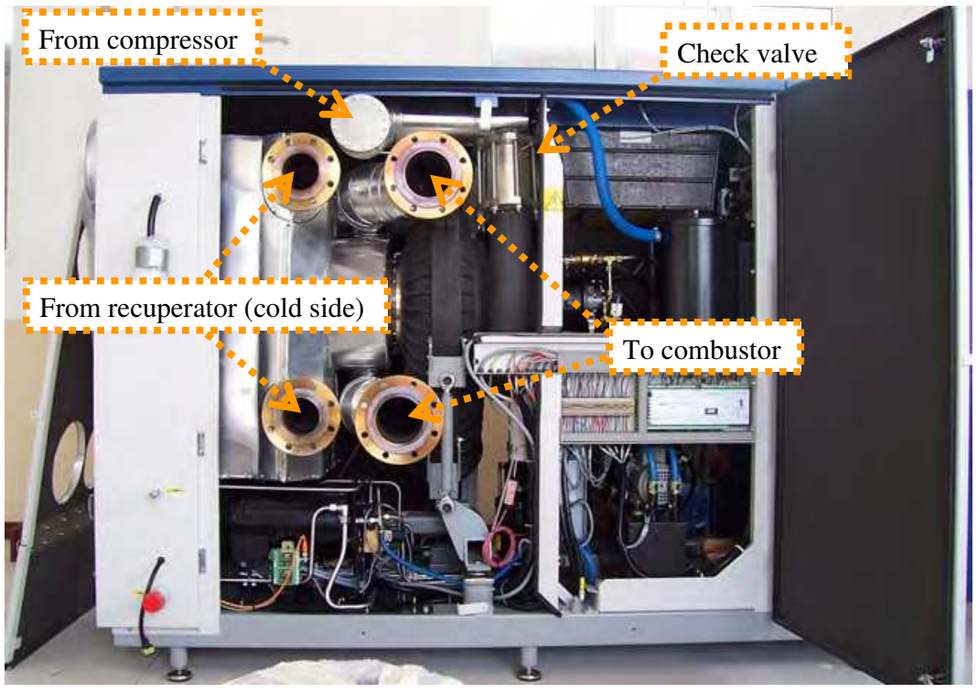

Fig. 3. T100 power module modified for coupling with the external pipe system.

The thermally insulated connection pipes are designed for high fidelity flow measurement, achieved with mass flow, pressure, and temperature probes, and flow management carried out with controlled valves. Moreover, these pipes were designed for easy connection to additional components between the compressor and expander, such as the modular vessel presented in the following paragraph. For this reasons, they merge the two flows at the recuperator outlets and split the combustor inlet flow for the connection to the two combustor pipes (see Figs. 3 and 4). Since this kind of mass flow measurements is carried out through pitot devices, each probe is preceded by a pipe of at least 18 diameter length and followed by a minimum length pipe of 4 diameters. This layout was chosen to obtain flow uniformity essential for high-precision measurements. A cold bypass was included to bypass the recuperator or connect the compressor outlet directly to additional external components (e.g. the modular vessel (Ferrari, 2009) used to emulate additional component dimensions). Moreover, the test rig includes a bleed line (Ferrari, 2009), equipped with a globe valve (VB), located at the compressor outlet. This device is essential to bleed part of

flow when operative conditions are too close to the surge region. An additional pipe, equipped with a mass flow rate meter was also installed to directly connect recuperator outlet to combustor inlet (through the VM valve), as in a typical recuperated cycle. These pipes are also essential in changing recuperator mass flow rate values.
The test rig was equipped with additional probes to measure the flow properties (Pascenti et al., 2007) (see Table 1). All additional transducers are connected to a PC, through a FieldPoint™ device, and their signals are acquired via LAN using a software developed in LabVIEW™ environment. These measurement devices are used to measure mass flow rates, pressures and temperatures inside the different lines of the plant. The locations of these probes are shown in the test rig layout diagram (Fig. 4). This plant layout refers to the machine working in the standard recuperated cycle (equipped with a check valve, a recuperator bypass, a bleed line, and additional probes).

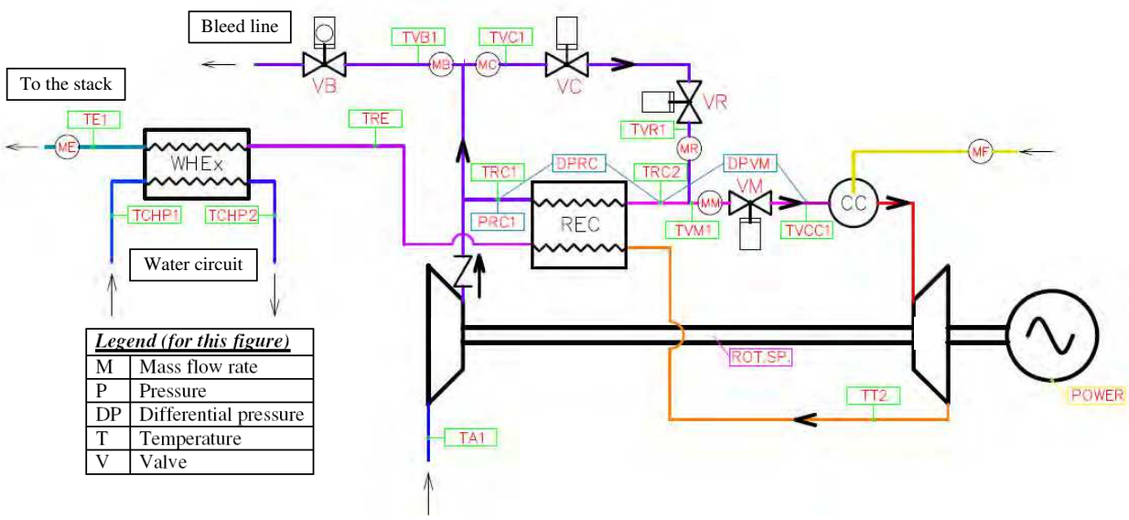

Fig. 4. Plant layout and instrumentation: machine and pipes (see Table 1 for the complete legend).

Since this machine is not designed for connection to additional components between the compressor and expander the connection pipes were developed to incur the lowest possible pressure drops. This is necessary to prevent surge conditions, and to avoid strong machine performance decrease. Therefore, gate valves were chosen (except in the case of the bleed line), and the pipes were designed with wide theoretical support.
A preliminary analysis was carried out with a test rig model in order to evaluate machine performance decrease (due to additional pressure and temperature losses), and to evaluate the operative limits. Then, a CFD analysis (see (Ferrari et al., 2007) for details) was performed with Fluent tool to verify the pipe design.
The test rig model was implemented with TRANSEO tool (in MATLAB®-Simulink® environment). This software (Traverso, 2005) is a simulation program based on an easy access library designed for the off-design, transient and dynamic analyses of advanced energy systems based on microturbine technology. TRANSEO was developed and validated at the University of Genoa in previous studies carried out by both Ph.D. students and TPG researchers (Caratozzolo et al., 2010; Ferrari et al., 2007; Traverso et al., 2005). After an experimental validation in design conditions (Ferrari et al., 2009a), the model was used to

calculate the operative curves (at constant TOT) on the compressor map (Fig. 5) at different pressure drop values (Δp) between recuperator and combustor. Each curve was calculated with a valve operating at fixed fractional opening. For this reason, Fig. 5 curves are obtained maintaining constant the ratio between the pressure drop (Δp) and the compressor outlet pressure (p_c). A maximum drop of 485 mbar was calculated at $\Delta p/p_c = 0.108$ to prevent any risk of surge (with the following surge margin limitation: K_p>1.1). To have a wide operative range, as required during the tests, a pressure drop limit of 300 mbar was calculated (the curve at $\Delta p/p_c = 0.069$ has a Δp = 290 mbar at 70000 rpm). These results were necessary to design pipes and valves with wide operative ranges during the tests and manage the rig under safe conditions. The nominal diameter values chosen for these pipes are: (i) 125 mm for the pipes immediately upstream of the combustor, (ii) 100 mm for the other connection pipes. The experimental tests showed good performance in agreement with the design target to obtain the lowest possible additional pressure drop (with the lowest space occupation too). The maximum pressure loss value (DPVM probe) measured during the tests is about 60 mbar.

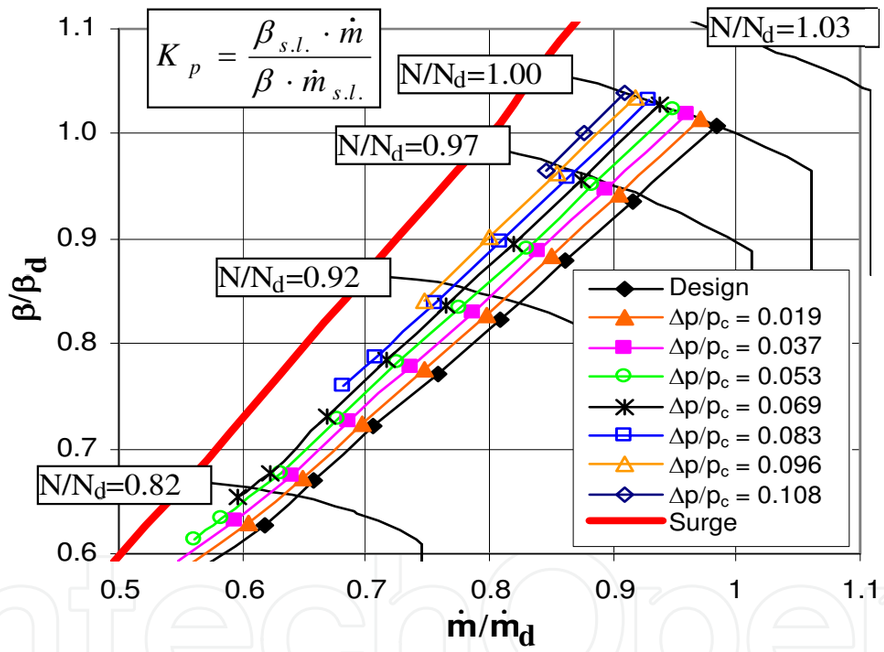

Fig. 5. Machine operation curves at constant $\Delta p/p_c$: TRANSEO model calculations.

4.1 Test example: Machine equipped with the external connection pipes

This paragraph shows an example of possible tests carried out on the machine equipped with the external pipes. For this reason Fig. 6 reports (on manufacturer compressor map) the experimental measurements carried out at different load values in stand-alone mode. These tests were performed using the compressor outlet pressure probe (PRC1 to measure the static wall pressure) and a mass flow meter (MM) located in the direct connection between the recuperator outlet and the combustor inlet (Fig. 4).

It is important to highlight these measurements, because they are essential for a correct theoretical analysis of the machine behaviour at both component and system levels and for a

complete model validation. While manufacturer compressor maps are usually essential for commercial machine models, this test rig allows to carry out wide experimental verification activities on these performance curves. Moreover, the experimental compressor maps are essential to prevent surge events during tests operated with external additional components (e.g. the modular vessel).

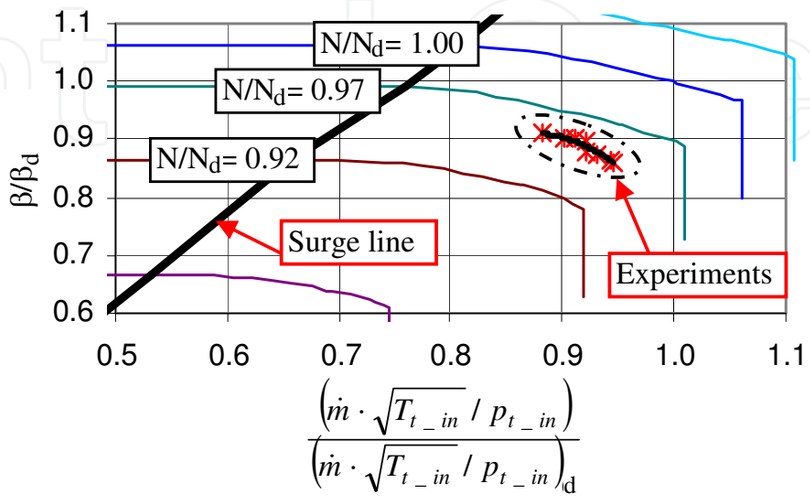

Fig. 6. Direct-line test: experimental data on compressor map obtained in stand-alone mode.

Since in stand-alone conditions the machine control system operates at constant rotational speed, it is possible to measure part of the curve at N/N_d=96.5. Within the accuracy of the probes utilized (Pascenti et al., 2007), the experimental points (Fig. 6) are well located between the 0.97 and 0.92 curves. The difference between the curve obtained from the manufacturer datum interpolation and the experimental points is due to the ambient temperature, which is around 25°C (298.15 K) instead of 15°C (288.15 K), and to the cited probe accuracy. However, ongoing works will be carried out to measure more map points, by converting the data into ISO conditions or operating at the ISO ambient temperature.

5. Machine connected to an external vessel

The machine operation with an additional volume located between compressor outlet and combustor inlet is typical of different innovative plant layout cycles (hybrid system, mHAT, externally fired cycle). This kind of volume is extremely significant on machine transient behaviour especially for plant component safety reasons (to avoid stress or dangerous conditions (Pascenti et al., 2007)). Therefore, this test rig was equipped with a modular vessel designed for experimental tests on the coupling of the machine with different kinds of components (e.g. saturators, fuel cells of different layouts or technology, or additional heat exchangers). The effect of these innovative components can be emulated through a right number of vessel modules to couple the real volume dimension with the micro gas turbine. The emulation of thermal and flow composition aspects can be carried out through the management of test rig valves (Ferrari et al., 2010a), the hardware/software coupling based on real-time models (Bagnasco, 2011), or the injection of additional flows (e.g. for the chemical composition emulation (Ferrari et al., 2011)).

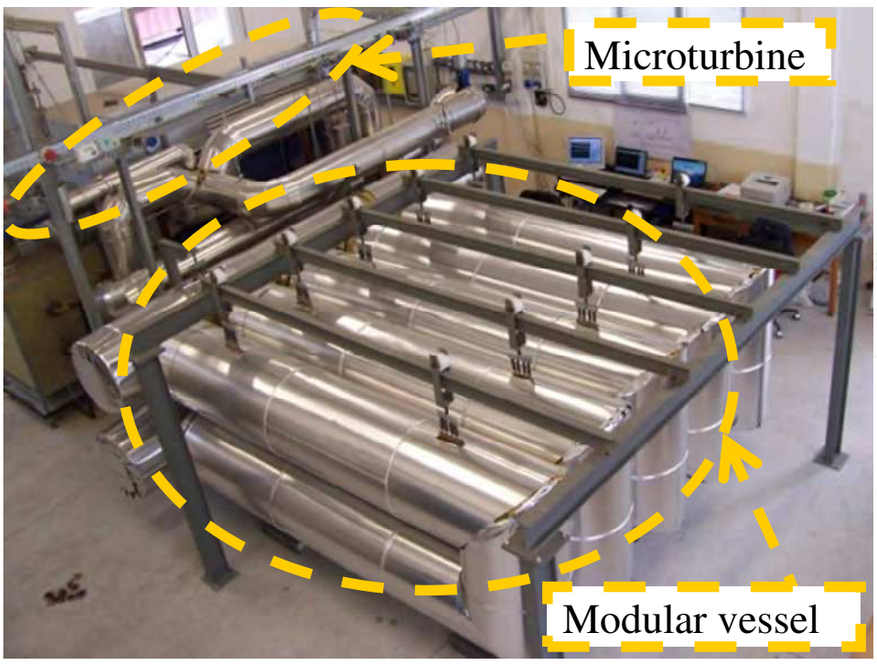

Fig. 7. Modular vessel coupled with the machine.

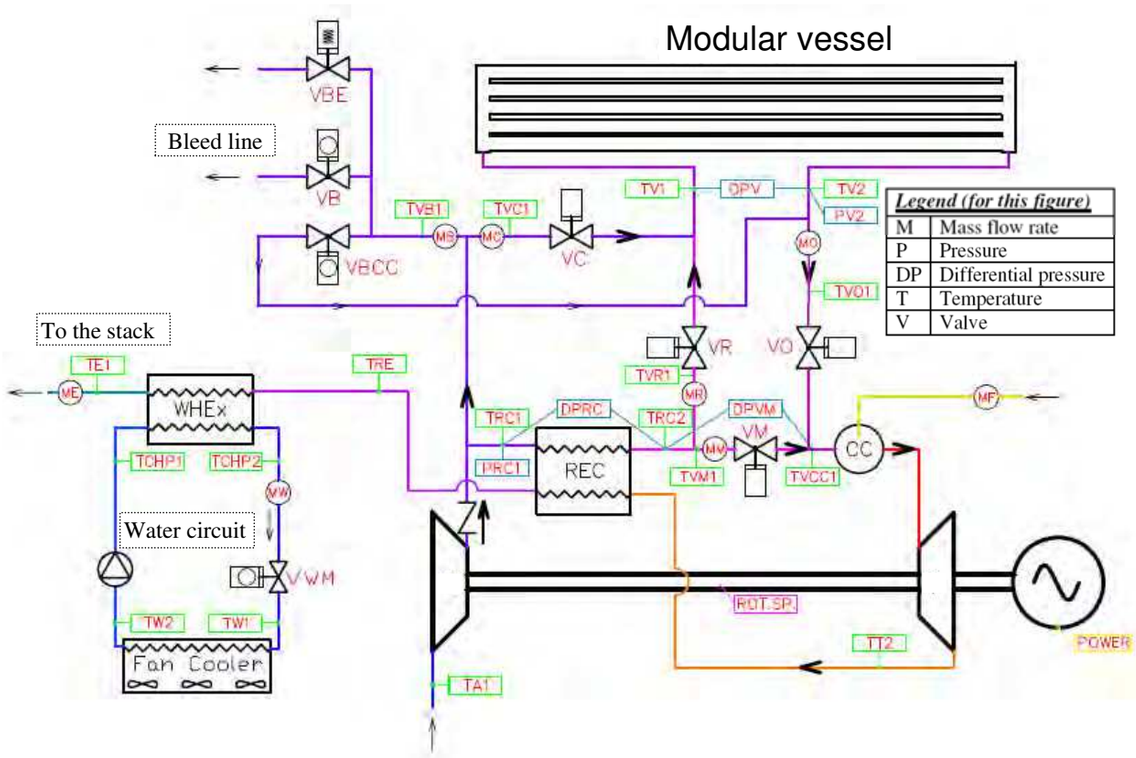

Fig. 8. Plant layout and instrumentation including the cathodic modular vessel (see Table 1 for the complete legend).

Mass flow rates			
Name	Location	Probe type	Accuracy
MM	Main line	Pitot tube	±1%
ME	Plant outlet	Thermal meter	±3%
MF	Fuel inlet	Thermal meter	±1%
MR	Vessel inlet from the recuperator	Pitot tube	±1%
MO	Vessel outlet	Pitot tube	±1%
MC	Vessel inlet from the compressor	Pitot tube	±1%
MB	Bleed outlet	Pitot tube	±1%
MW	Water main line	Magnetic meter	±4%
Static pressures			
Name	Location	Probe type	Accuracy
PA1	Ambient	Ambient sensor	±1%
PRC1	Recuperator inlet	Absolute	±1%
DPRC	Recuperator loss	Differential	±1%
DPVM	Main line loss	Differential	±1%
DPV	Vessel loss	Differential	±1%
PV2	Vessel outlet	Absolute	±1%
Temperatures			
Name	Location	Probe type	Accuracy
TA1	Ambient	Ambient sensor	±1%
TRC1	Recuperator inlet	Thermocouple	±2.5 K
TRC2	Recuperator outlet	Thermocouple	±2.5 K
TVM1	Main line pitot	Thermocouple	±2.5 K
TVCC1	Combustor inlet	Thermocouple	±2.5 K
TT2	Turbine outlet	Thermocouple	±2.5 K
TE1	Plant outlet	Thermocouple	±2.5 K
TVR1	From the recuperator pitot	Thermocouple	±2.5 K
TV1	Vessel inlet	Thermocouple	±2.5 K
TV2	Vessel outlet	Thermocouple	±2.5 K
TVO1	From the vessel pitot	Thermocouple	±2.5 K
TVC1	From the compressor pitot	Thermocouple	±2.5 K
TVB1	Bleed valve inlet	Thermocouple	±2.5 K
TCHP1	WHEx inlet	PT100 RTD	±0.3 K
TCHP2	WHEx outlet	PT100 RTD	±0.3 K
TC1	Compressor inlet	PT100 RTD	±0.3 K
TRE	Recuperator outlet	Thermocouple	±2.5 K
TW1	Cooler inlet	PT100 RTD	±0.3 K
TW2	Cooler outlet	PT100 RTD	±0.3 K

Table 1. Additional probes referred to Fig. 10 layout.

The vessel is composed of two collector pipes, connected to the recuperator outlet and the combustor inlet respectively (see Figs. 7 and 8), and five module pipes connected to both collectors. Both collectors and module pipes have a nominal diameter of 350 millimetres and their total length is around 43 meters for a maximum volume of about 4 m^3. This vessel can emulate the volume of additional components suitable for the machine size.

Figure 8 shows the rig layout with the modular vessel and all the additional probes and valves introduced in this plant configuration (see Table 1 for further instrumentation details). In comparison with the layout shown in Fig. 4, a vessel outlet line equipped with a gate valve (VO) was installed, a bleed emergency valve (VBE) was included to prevent surges during emergency shutdown, and an additional globe pneumatic valve (VBCC) was introduced to connect the compressor outlet directly to the combustor inlet. Moreover, the test rig was further improved with the installation of a water fan cooler located outside of the laboratory. It is based on three 0.7 kW electrical fans used to cool down the water (coming from the WHEx of Fig. 8), and to operate in closed circuit conditions (a 1.5 kW variable speed pump was installed).

6. Hybrid system emulation devices

To perform tests related on high temperature fuel cell hybrid systems a part of the external vessel (collectors and four modules) is used to emulate the cathodic dimension of a fuel cell stack. For this reason, the maximum cathodic volume is about 3.2 m^3. The fifth vessel module is used to emulate the related anodic volume (about 0.8 m^3) and an ejector (Ferrari et al., 2006) based anodic recirculation was included in the rig. Moreover, this facility was equipped with a steam injection system to emulate the turbine inlet composition typical of a hybrid system and a real-time model was connected to the plant for components not physically present in the rig. All these emulation devices were designed to analyse a SOFC based hybrid system of 450 kW electrical load (consistent with the machine size) (Ferrari et al., 2009a) scaled on the basis of the Rolls-Royce Fuel Cell Systems (RRFCS) planar stack (size: 250 kW; fuel utilization: 75%; stack temperatures: 800-970°C; current density: 2940 A/m^2) (Massardo & Magistri, 2003). The layout of the test rig equipped with the anodic recirculation and the steam injection systems is shown in Fig. 9.

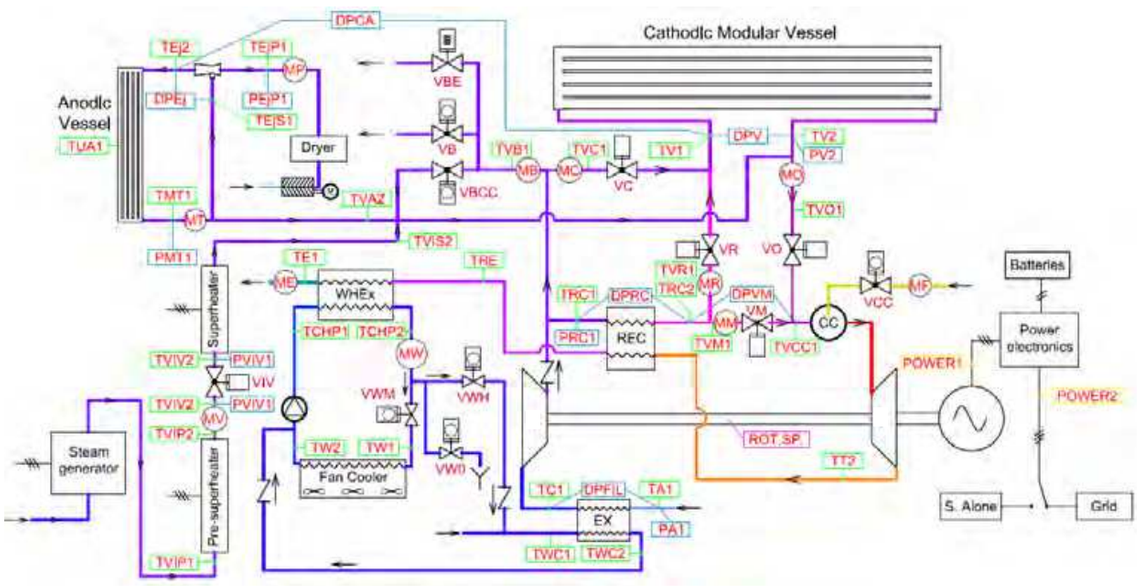

Fig. 9. Plant layout and instrumentation including the anodic recirculation and the steam injection systems.

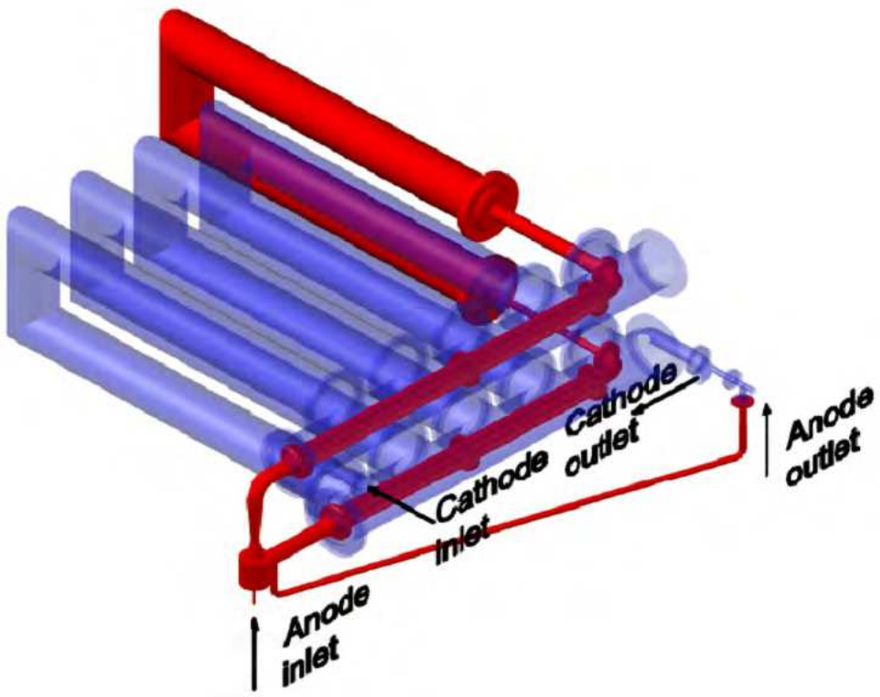

Fig. 10. The anodic loop layout.

6.1 The anodic recirculation and the steam injection systems

The anodic recirculation system (Fig. 10) is composed of a compressed air line (for fuel flow emulation), an anodic single stage ejector, and an anodic vessel. The compressed air line was designed to supply the ejector primary duct with an air mass flow rate up to 20 g/s (Ferrari et al., 2009b). This approach was developed to emulate the fuel mass flow rate at the ejector primary duct with an air mass flow rate. The anodic ejector generates the recirculation flow rate through this system as in a typical SOFC hybrid system. The 0.8 m^3 anodic vessel was designed to heat up the flow in the anodic loop. For this reason, to better emulate the anodic side, a pipe based heat exchanger was developed as shown in (Ferrari et al., 2010b). To better show this layout, a 3-D CAD plot (Fig. 10) was developed: part of the anodic loop was inserted into the cathodic vessel to partially heat the anodic flow.

The steam injection system was designed to obtain at the expander inlet the same c_p value of the reference hybrid system. This similitude approach is completely explained in (Ferrari et al., 2011). For this reason the rig was equipped with a 120 kW electrical steam generator capable of at least 27 g/s, a 40 kW electrical super-heater to increase the steam temperature from the steam generator outlet condition to a temperature suitable for the turbine combustor inlet (around 515°C), and a controlled valve for the mass flow rate management. The measuring of the steam flow rate requires a completely mono-phase steam. So upstream of the mass flow probe, an additional electrical heater (called Pre-superheater) was installed. Furthermore, several thermocouples were added for control and diagnostic purposes. The final layout is shown in Fig. 9.

All the additional probes included in the rig for these additional hardware devices (anodic recirculation and steam injection systems) are reported in Tab. 2.

Mass flow rates			
Name	Location	Probe type	Accuracy
MP	Ejector primary line	Thermal meter	±1%
MT	Anodic volume line	Venturimeter	±3%
MV	Steam generator outlet	Vortex meter	±1%
Static pressures			
Name	Location	Probe type	Accuracy
PEjP1	Ejector primary duct inlet	Absolute	±1%
PMT1	Anodic volume line	Absolute	±1%
DPEj	Anodic ejector	Differential	±1%
DPCA	Cathodic/Anodic circuit pressure difference	Differential	±1%
PVIV1	Steam control valve inlet	Absolute	±1%
PVIV2	Steam control valve outlet	Absolute	±1%
Temperatures			
Name	Location	Probe type	Accuracy
TEjP1	Ejector primary duct inlet	Thermocouple	±2.5 K
TEjS1	Ejector secondary duct inlet	Thermocouple	±2.5 K
TEjS2	Ejector outlet	Thermocouple	±2.5 K
TUA1	Anodic volume (U pipe inlet)	Thermocouple	±2.5 K
TMT1	Anodic flow venturimeter	Thermocouple	±2.5 K
TVA2	Anodic circuit outlet	Thermocouple	±2.5 K
TVIP1	Steam generator outlet	Thermocouple	±2.5 K
TVIP2	Pre-superheater generator outlet	Thermocouple	±2.5 K
TVIV1	Steam control valve inlet	Thermocouple	±2.5 K
TVIV2	Steam control valve outlet	Thermocouple	±2.5 K
TVIS2	Steam system outlet	Thermocouple	±2.5 K

Table 2. Additional probes (not shown in Fig. 8 layout) referred to Fig. 9.

6.2 Fuel cell stack real-time model to be connected to the rig

To complete the emulation of a SOFC hybrid system a real-time model was developed in Matlab®-Simulink® to be coupled to the experimental test rig. This model (developed with components validated in previous works (Ghigliazza et al., 2009a; Ghigliazza et al., 2009b) was based on the simplification of simulation components (cell stack, reformer, anodic loop, off-gas burner, expander) developed in the TRANSEO tool (Traverso, 2005) of the TPG research group. Through the Real-Time Windows Target tool and the UDP interface approach it is possible to study the entire hybrid system using the model for components not physically present in the test rig.

Figure 11 shows how the real-time model and the experimental facility are connected to emulate the entire hybrid system. The real-time model receives (as inputs) the mass flow rate, the pressure and the temperature values at the machine combustor inlet level. Furthermore, it receives the machine rotational speed and the acquisition time values. These input data are transferred from LabVIEW™ software to the real-time model (in Simulink®) through an apt UDP interface. The real-time model is used to calculate the fuel cell system

behaviour over time. In detail, this model is composed of a reformer, a SOFC stack, an off-gas burner, an anodic ejector based recirculation system, a cathodic blower based recirculation, and the expander of the T100 machine. So, in this work this real-time model is used to calculate the TOT values coming from an interaction between the SOFC system and the T100 expander. This TOT value is used over time to control the real machine (the electrical load in stand-alone mode) to produce the same TOT value of the model. Also this output interface is managed through the UDP approach. Moreover, the interface includes a port to transfer to LabVIEW™ software the mass flow rate values of anodic ejector primary duct (MP). This values are used to carried out tests with the MP mass flow rate equal to the fuel flow calculated in the model. With this hardware/software interconnection layout it is possible to emulate the stack/turbine interaction from an experimental point of view studying different operative conditions.

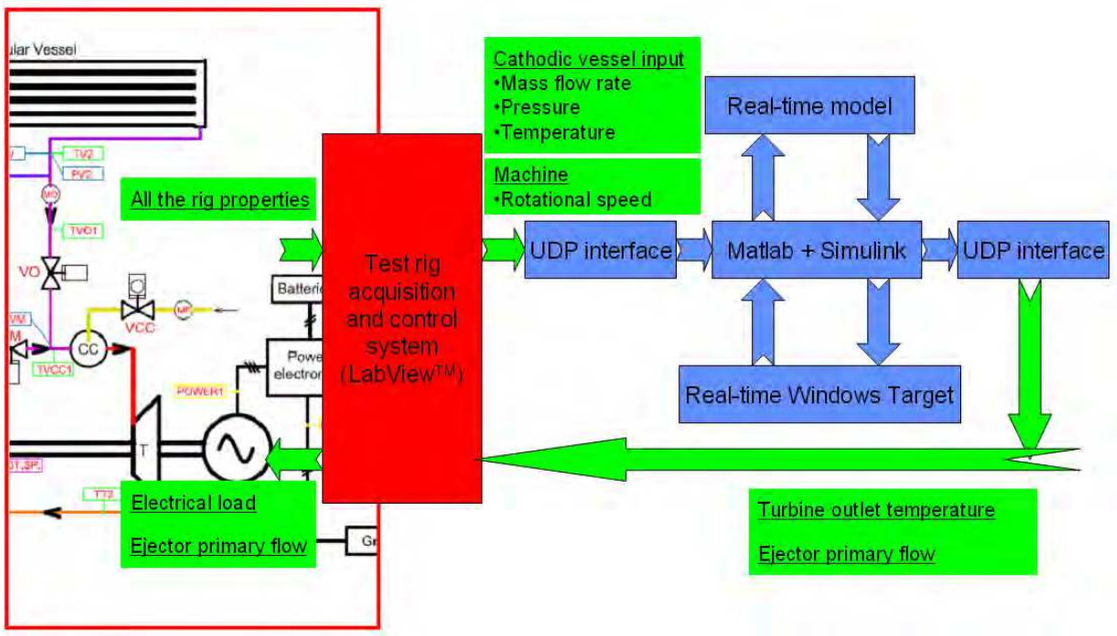

Fig. 11. Hybrid system emulation: hardware/software interconnection layout.

6.2.1 Test example: Hybrid system emulation

This paragraph reports an example of possible tests to be carried out with these emulator devices. This test was performed according to the following procedure:

1. establish connection between the real-time model and the plant;
2. impose requested current and fuel variation on model user interface;
3. the model simulates in real-time mode the evolution of SOFC properties towards a new operative point;
4. the calculated values of TOT and anodic ejector primary flow are continuously fed to the plant control system as set point values;
5. the control system moves machine load until the measured TOT value is equal to the calculated one, and operates on the MP control valve to generate flow values coming from the model.

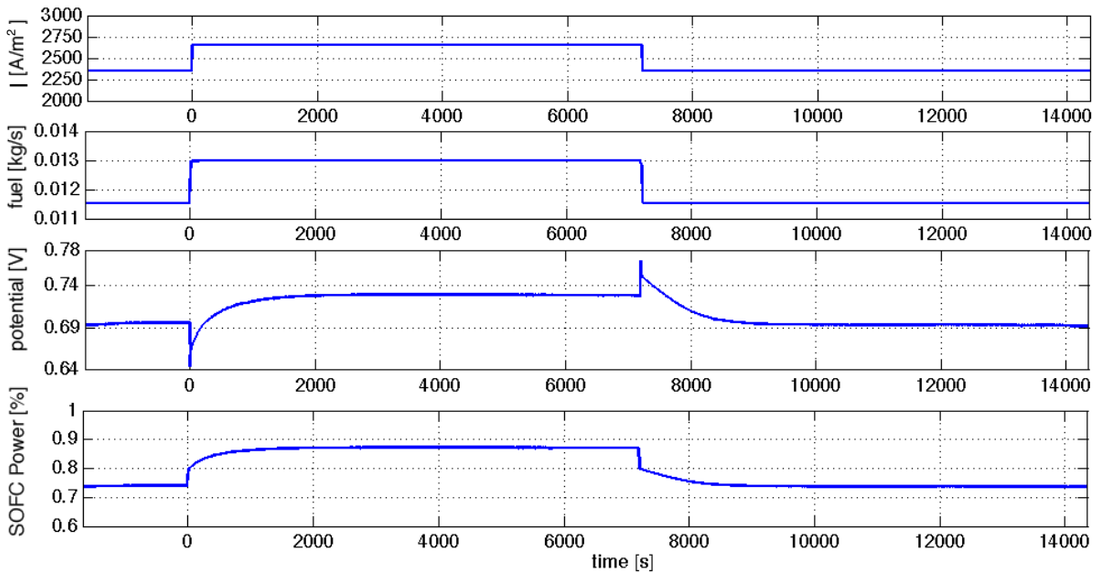

Fig. 12. Emulation test with the real-time model: current density (I), fuel mass flow rate, cell potential, SOFC power (referred to its design value).

The test is based on a concurrent variation of SOFC drawn current and mass flow rate of anodic ejector fuel. From a steady-state condition, corresponding to 80% of nominal current and primary fuel flow, the model performed a step increase in both parameters to 90% of nominal values. When a new steady-state condition (about 2 hours) was reached the model brought back the system to the initial condition. Figure 12 shows the trend of steps related to the input parameters. Moreover, the behaviour of single cell potential, and SOFC total electric power (AC) are reported. Both properties show an initial step variation, due to the input steps, followed by a long duration variation due to the SOFC temperature behaviour over time (high thermal capacitance of the SOFC). In detail, the cell voltage increases when the SOFC temperature increases for the electrical losses decrease (see (Bagnasco, 2011) for further details).

Figure 13 shows the trend of measured turbine outlet temperature and the calculated turbine inlet temperature values: it can be easily noticed how the TOT signal is affected by a constant noise characteristic of values coming from field while the TIT (calculated) shows a smoother behaviour. These values increase with the current and fuel increase (SOFC temperature increase). Figure 13 also shows the variation of the utilization factor (Eq. 1) and hybrid system (HS) global efficiency (Eq. 2). The U_f peak is due to the fluid dynamic delay between the current variation (instantaneous) and the fuel change on the stack. The hybrid system efficiency shows the step effect followed by a long time variation due to thermal aspects. The global efficiency oscillation, with high peaks in the area after the second step (7500-8000 s), are due to unexpected fuel flow discontinuities during the test.

$$U_f = \frac{\left[nH_2\right]_{cons}}{\left[4 \cdot nCH_4 + 6 \cdot nC_2H_6\right]_{in}} \tag{1}$$

$$\eta_{HS} = \frac{P_{GT} + P_{FC} - P_{blower}}{\dot{m}_{fuel}} \tag{2}$$

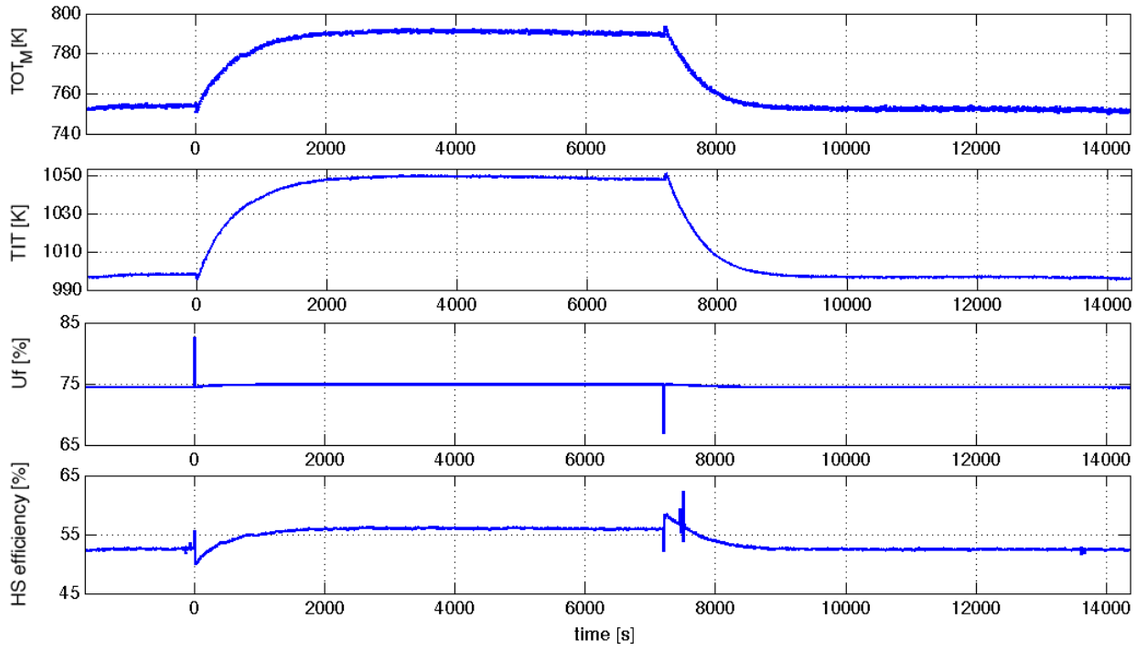

Fig. 13. Emulation test with the real-time model: measured turbine outlet temperature (TOT_M), turbine inlet temperature (TIT), fuel utilization factor, hybrid system efficiency.

7. Compressor inlet temperature control devices

A new water system was designed and installed to control the machine compressor inlet temperature (Fig. 9 layout). This system is composed of three air/water heat exchangers installed at the machine air intakes (Fig. 14) and connected to the water system. Even if the water pipe layout was modified for the connection with an absorption cooler (see the following paragraph), this part of the paper describes the previous rig layout that was used for a wide experimental campaign carried out on the machine recuperator. In this past configuration, the water system was equipped with three controlled electrical valves (VWM, VWH, and VWO of Fig. 9). It was possible to cool down the compressor inlet air by means of cold water from the supply system (opening VWO), and to heat up this air flow (closing VWM, and opening VWH) by means of the hot water coming from the machine co-generation system (WHEx). A new control system (see (Ferrari et al., 2010c) for details) was developed to manage these valves for the required temperature generation. With this past layout, maximum cooling performance depended on the supply water temperature (about 22°C in summer, that is 295.15 K), while the only restriction for heating performance is the maximum compressor inlet air temperature for the machine cooling system, that is 40°C (313.15 K). However, in the following paragraph, it is possible to notice that an absorber cooler connected to the system allows to study tri-generation options and use the produced cold flow for higher compressor inlet temperature cooling.

7.1 Test example: compressor inlet temperature control

As an example of possible tests to be carried out with the compressor inlet temperature control devices, this paragraph shows the experimental data measured on the recuperator of this test rig when operating in the machine standard layout. Since the large influence on the

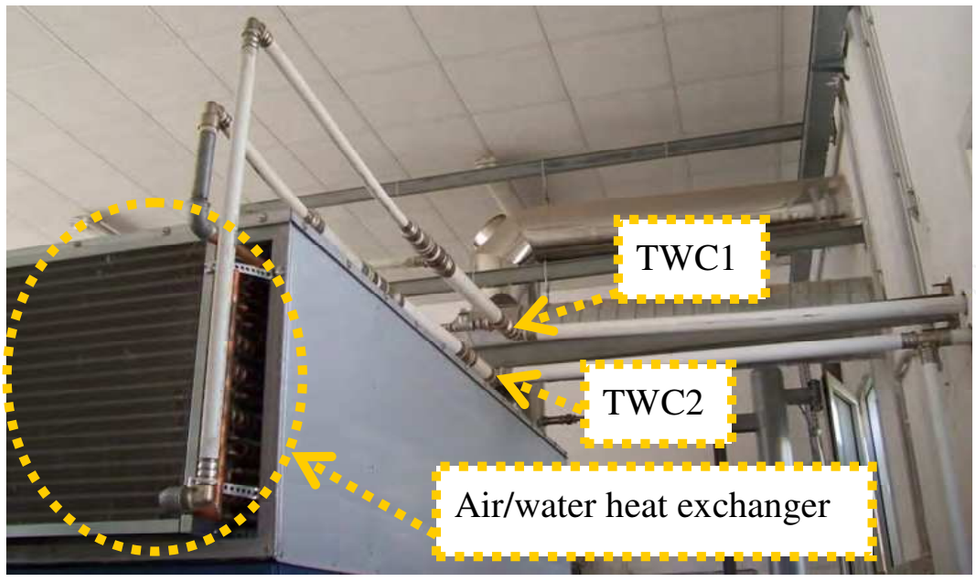

Fig. 14. An air/water heat exchanger with water pipes for compressor inlet temperature control.

recuperator temperatures of the compressor inlet temperature, this new control system was used to maintain this temperature at a fixed value of 28°C (301.15 K, with maximum errors of ±0.3 K during all the tests). These steady-state tests were carried out with the machine connected to the electrical grid to measure recuperator performance at different mass flow rate values. In this configuration the machine control system operates at constant TOT (called TT2 in Fig. 9, that is maintained at 645°C (918.15 K)) and changes the rotational speed (and the air mass flow rate) with load changes. For surge prevention purposes, it is not possible to perform tests below a 20 kW electrical load. After the machine heating phase (during the start-up), the controller does not accept load values below 20 kW.

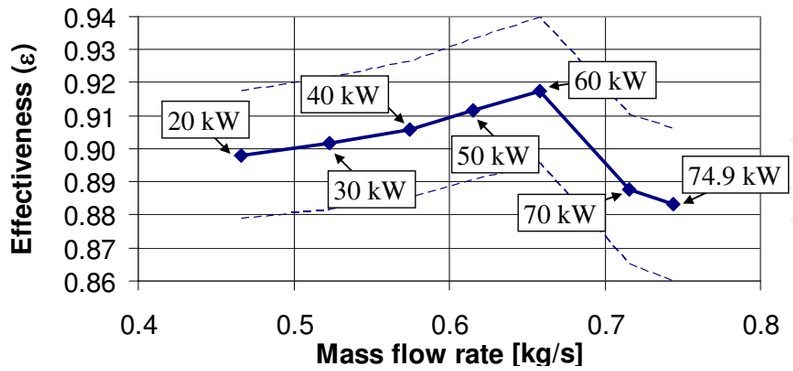

Fig. 15. Steady-state recuperator effectiveness obtained from experimental data at different loads (machine connected to the electrical grid).

Figure 15 shows the recuperator effectiveness (defined in Eq. 3 with Fig. 9 nomenclature) obtained at different electrical load values, i.e. different air mass flow rates. While the continuous line connects the effectiveness values calculated through recuperator boundary temperatures (measured during the tests), the dotted lines show the accuracy values

(around ±2%) of this performance parameter. This uncertainty band was calculated through temperature measurements affected by a ±2.5 K accuracy. As shown in previous theoretical works (e.g. (McDonald, 2003)), starting from maximum flow it is possible to observe an effectiveness increase (from 0.883 to 0.918) with the mass flow rate decrease, and an effectiveness maximum followed by a decrease. However, this final trend is not so relevant as in (McDonald, 2003), because machine control system does not enable to operate steady-state tests under 20 kW (under 0.47 kg/s). Further details on all the recuperator temperatures and other tests carried out on this heat exchanger, when operating with the T100 modified machine, are shown in (Ferrari et al., 2010c).

$$\varepsilon = \frac{TRC2 - TRC1}{TT2 - TRC1} \tag{3}$$

8. Test rig integration with an absorber cooler unit

To carry out tests at compressor inlet temperature values under 20°C and to study tri-generative configurations, the facility was equipped with an absorber cooler. This device exploits the thermal content of machine exhaust flow (water at 95°C, that means 368.15 K, produced by the WHEx of Fig. 9) to produce cold water (7-12°C, that means 280.15-285.15 K). This refrigeration energy is essential for the machine inlet and for the laboratory cooling during summer or long time tests.

As shown in Fig. 16 the machine produces, in full load conditions, about 113 kW of thermal power to obtain about 2 l/s of hot water at 95°C (the system operates in closed circuit configuration). With this thermal power the absorber is able to generate about 80 kW of cooling power. This system is based on an absorber inverse cycle (water/lithium bromide) operating (in the test rig conditions) at a 0.7 COP value.

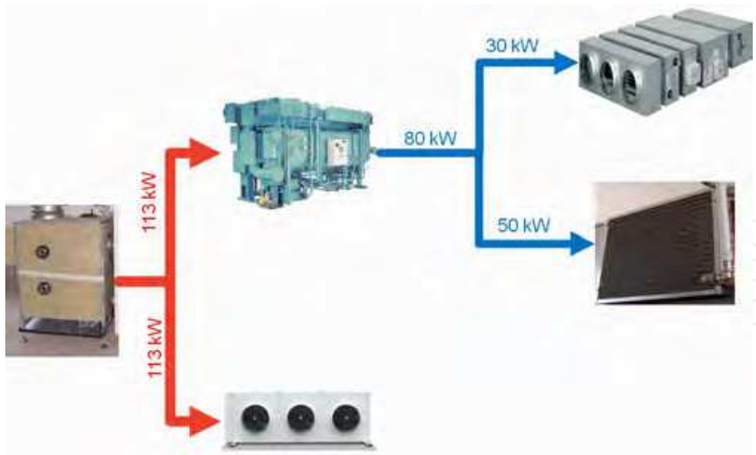

Fig. 16. Maximum thermal power related to both heating and cooling.

The water plant (modified in comparison with Fig. 9) related to refrigeration was designed for a maximum 50 kW cold power for the compressor inlet cooling and 30 kW (at maximum) for the laboratory conditioning. Moreover, with the "Fan Cooler" water/air heat exchanger (already shown in Fig. 9) it is possible to emulate a heating system using a part of the 113 kW thermal power, operating in tri-generative condition. So, While the "Fan Cooler"

is used to emulate a heating system, the heat exchangers used to manage the cold power are essential to emulate a cold thermal load.
Figure 17 shows the plant scheme related to cold water generation (from the absorber unit) and thermal power management. For this new water plant three pumps were installed: 1.5 kW pump for the hot water (2 l/s mass flow rate, 2.45 bar pressure increase), 7.5 kW pump for the cold water (5 l/s mass flow rate, 8.34 bar pressure increase), and a third pump (5.5 kW) to refrigerate the condenser of the absorber unit (12 l/s mass flow rate, 2.74 bar pressure increase). A 260 kW evaporative tower was installed for the refrigeration water (see (Prando et al., 2010) for further details). To operate the laboratory cooling a 20 kW water/air heat exchanger was designed and installed in the rig. Moreover, to perform heating conditions at the compressor inlet level, as already included in the previous facility configuration, (for instance for the emulation of a summer performance during winter) a water/water heat exchanger was included. It is a plate exchanger (power: 80 kW, primary flow: 1.44 l/s, secondary flow: 5 l/s) used to heat the "Ex" water directly with the hot water from the "WHEx" (see Fig. 17 for layout details). The water plant was also equipped with controlled valves for flow management and with mass flow rate (Magnetic meter - accuracy: ±4%) and temperature (PT100 RTD - accuracy: ±0.3 K) probes for measurement of main properties (see (Prando et al., 2010) for further details).

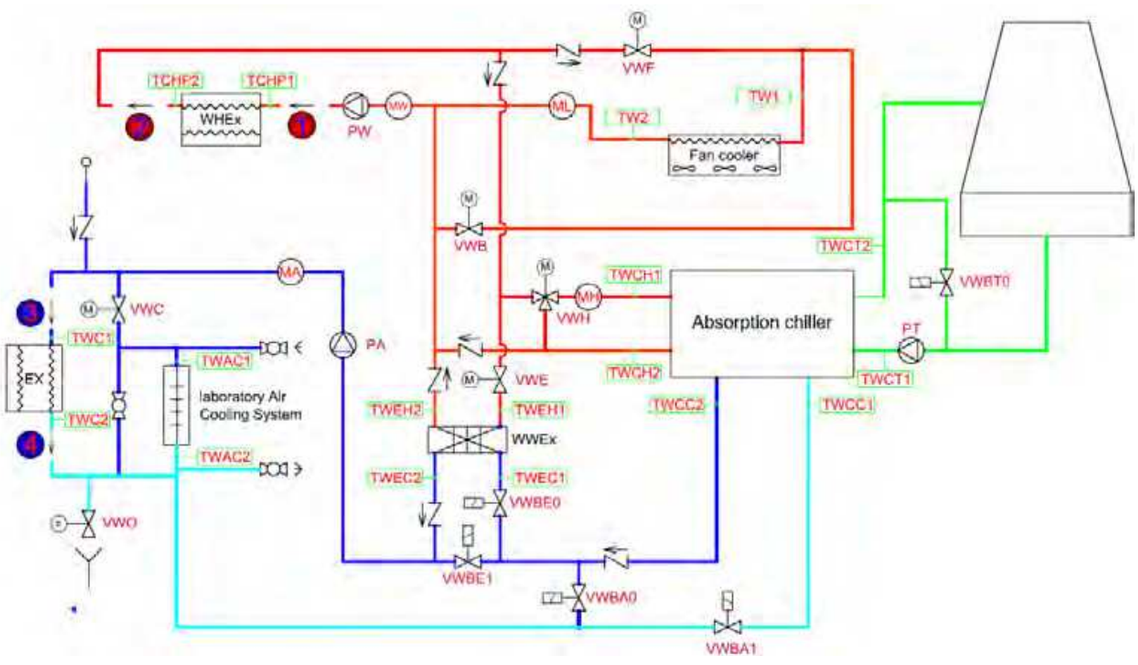

Fig. 17. Water system plant layout for the tests with absorber unit.

9. Model validation activities

Great attention is devoted to this activity to validate time-dependent simulation models at both component (recuperator) and system (the hybrid system emulator test rig) levels. A good level of consistency can be achieved thanks to the complete knowledge of the test rig dimensions, volumes, masses, shaft inertia, thermal capacitances, and operating procedure. Such completeness is difficult to obtain in industrial plants, where details about equipment

are often missing or confidential. The following paragraph shows an example of this kind of validation activities focusing the attention on the machine recuperator.

9.1 Test example: The recuperator model

This validation activity regards the primary-surface (cube geometry) recuperator located inside the power case of the Turbec T100 machine (Turbec, 2002). So, a recuperator real-time model was tested against experimental data not in a heat exchanger test rig, but in a real operative configuration, working in a commercial recuperated 100 kWe machine. The recuperator model adopts the lumped-volume approach (Ferrari et al., 2005) for both hot and cold flows. Since momentum equation generates negligible contribution during long-time transients, because it produces quite fast effects (dynamic effects) that are negligible in a component with average flow velocities at around 10 m/s, it is possible to properly represent the transient behaviour of the heat exchanger just using the unsteady form of the energy equation (the actual governing equation (Ghigliazza et al., 2009a) of the system).

The finite difference mathematical scheme (shown in Fig. 18) is based on a recuperator division into four main parts (j = 0, 1, 2, 3). The internal grid is "staggered" to model the heat exchange between each solid cell (j = 1, 3) and the average temperature of the flow (j = 0, 2): M+1 faces correspond to M cells. The resulting quasi-2-D approach is considered a good compromise between accuracy of results and calculation effort. The heat loss to environment and the longitudinal conductivity into solid parts are also included. All the equations and the integration approach of this model are described in (Ghigliazza et al., 2009a). Moreover, this paper reports the main data used for the recuperator model (Table 3) for the results reported here.

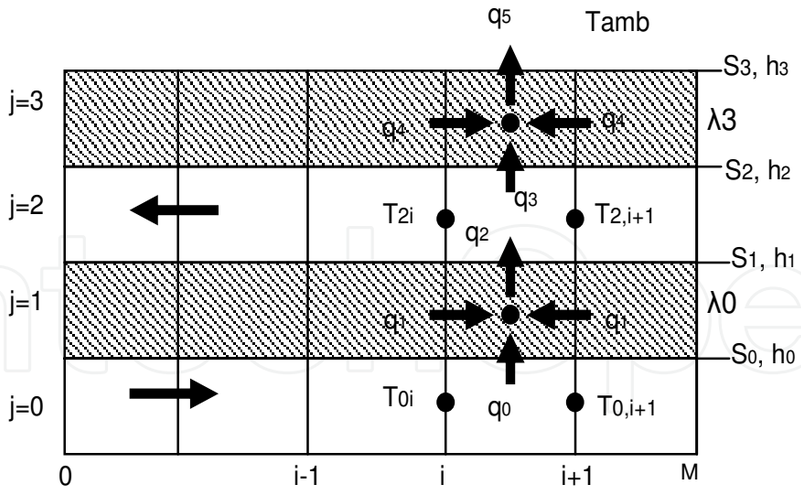

Fig. 18. Real-time model: finite difference scheme.

Figure 19 shows the comparison between experimental data and model results related to recuperator outlet temperature (cold side). The test considered here is a machine start-up phase carried out from cold condition. The results obtained during this test are acceptable, even if same margin of improvement exists. With reference to Fig. 19, the following aspects can be highlighted:

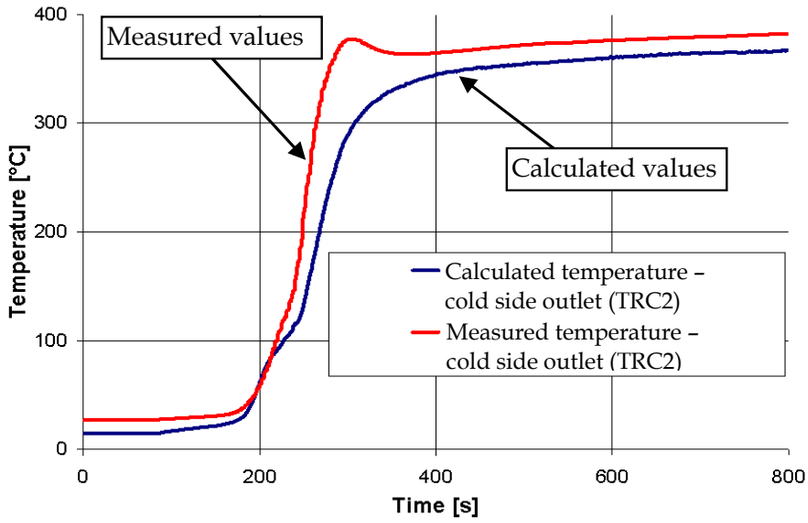

Fig. 19. Recuperator model validation (start-up phase): cold side outlet.

Thermal capacitance	226.05 [kJ/K]
Convective heat exchange (cold side)	500 [W/m²K]
Convective heat exchange (hot side)	250 [W/m²K]
Length	0.35 [m]
Nominal pressure drop (cold side)	0.06 [bar]
Nominal pressure drop (hot side)	0.06 [bar]

Table 3. Recuperator model data.

- the matching between measured data and model predictions is within a difference of 50°C, which can be considered a good result considering real-time simulation performance;
- measurements show a longer thermal delay (likely explanation: effect due to thermal shield of thermocouples).

10. Conclusion

A new test rig based on micro gas turbine technology was developed at the TPG laboratory (campus located at Savona) of the University of Genoa, Italy. It is based on the coupling of different equipments to study advanced cycles from experimental point of view and to provide students with a wide access to energy system technology. Particular attention is devoted on tests related on hybrid systems based on high temperature fuel cells. The main experimental facilities developed and built for both student and researcher activities are:

- A commercial recuperated micro gas turbine (100 kW nominal electrical load) equipped with a hot water co-generation unit and with the essential instrumentation for control reasons and to operate typical tests (start-up, shutdown, load changes) on the machine.
- A set of external pipes connected to the machine for the flow measurement and management. These pipes are used to measure with enough accuracy all the properties necessary for cycle characterization (e.g. the air mass flow rate or recuperator boundary

temperatures), not available in the machine commercial layout. In particular the chapter shows a test example related to the compressor map measuring.
- An external modular vessel to test the coupling of the machine with different additional innovative cycle components, such as saturators, fuel cells of different layouts or technology, or additional heat exchangers.
- Additional devices for hybrid system emulation activities. This part describes the anodic recirculation based on a single stage ejector (coupled to the rig for tests related to the anodic/cathodic side interaction), the steam injection system based on a 120 kW steam generator (used to emulate the turbine inlet composition typical of a hybrid system), and a real-time model used to emulate the components not physically present in the rig (e.g. the fuel cell). As an example of tests carried out with these devices, this chapter reports the main results obtained during fuel and current steps carried out with the real-time model coupled with the rig.
- Compressor inlet temperature control devices (heat exchangers, pipes, pump, and control system) to evaluate performance variations related to ambient temperature changes. Particular attention is focused on tests carried out on the recuperator with the machine operating in grid-connected conditions.
- An absorber unit connected to the plant (the hot water generated by the WHEx is used as primary energy to produce cold water) to carry out tests at compressor inlet temperature values under 20°C and to study tri-generative configurations.
- Great attention is devoted to validation activities for time-dependent simulation models. As an example, this chapter shows the comparison between experimental data and model results related to recuperator outlet temperature (cold side), during a cold start-up phase.

Besides the additional developments and tests on the rig, already planned and presented in (Pascenti et al, 2007; Ferrari et al., 2009a; Ferrari et al., 2010c; Prando et al., 2010), all the different layout configurations will be considered for tests. For instance, in an ongoing work it is planned to use the real-time model for control system development activities related on SOFC hybrid plants and the absorber cooler to carry out tests at lower ambient temperature conditions, also considering tri-generative configurations.

11. Acknowledgment

This test rig was mainly funded by FELICITAS European Integrated contract (TIP4-CT-2005-516270), coordinated by Fraunhofer Institute, by LARGE-SOFC European Integrated Project (No. 019739), coordinated by VTT, and by a FISR National contract, coordinated by Prof. Aristide F. Massardo of the University of Genoa.
The authors would like to thank Prof. Aristide F. Massardo (TPG Coordinator) for his essential scientific support, Dr. Loredana Magistri, (permanent researcher at TPG) for her activities in design point definition, and Mr. Alberto N. Traverso (associate researcher at TPG) for his technological support on absorption cooler installation.

12. References

Kolanowski, B. F. (2004). *Guide to Microturbines*, Fairmont Press, ISBN 0824740017, Lilburn, Georgia (USA).

Boyce, M. P. (2010). Handbook for Cogeneration and Combined Cycle Power Plants, Second Edition, ASME Press, ISBN 9780791859537, New York, New York (USA).

Massardo, A. F., McDonald, C. F., & Korakianitis, T. (2002). Microturbine-Fuel Cell Coupling for High-Efficiency Electrical-Power Generation. Journal of Engineering for Gas Turbines and Power, Vol. 124(1), pp. 110-116, ISSN 0742-4795.

Lindquist, T., Thern, M., Torisson, T. (2002). Experimental and Theoretical Results of a Humidification Tower in an Evaporative Gas Turbine Cycle Power Plant. *Proceedings of ASME Turbo Expo 2002*, 2002-GT-30127, ISBN 0791836010, Amsterdam, The Netherlands, June 3-6, 2002.

Traverso, A., Massardo, A. F., Scarpellini, R. (2006). Externally Fired micro-Gas Turbine: Modelling and Experimental Performance. *Applied Thermal Engineering*, Elsevier Science, Vol. 26, pp. 1935-1941, ISSN 1359-4311.

Magistri, L., Costamagna, P., Massardo, A. F., Rodgers, C., McDonald, C. F. (2002). A Hybrid System Based on a Personal Turbine (5 kW) and a Solid Oxide Fuel Cell Stack: A Flexible and High Efficiency Energy Concept for the Distributed Power Market, *Journal of Engineering for Gas Turbines and Power*, Vol. 124, pp. 850-875, ISSN: 0742-4795, New York, New York (USA).

Magistri, L., Traverso, A., Cerutti, F., Bozzolo, M., Costamagna, P., Massardo, A. F. (2005). Modelling of Pressurised Hybrid Systems Based on Integrated Planar Solid Oxide Fuel Cell (IP-SOFC) Technology. *Fuel Cells*, Topical Issue "Modelling of Fuel Cell Systems", WILEY-VCH, Vol. 1, Issue 5, ISSN 1615-6854.

Pedemonte, A. A., Traverso, A., Massardo, A. F. (2007). Experimental Analysis of Pressurised Humidification Tower For Humid Air Gas Turbine Cycles. Part A: Experimental Campaign. *Applied Thermal Engineering*, Elsevier Science, Vol. 28, pp. 1711–1725, ISSN 1359-4311.

McDonald, C. F. (2003). Recuperator Considerations For Future High Efficiency Microturbines. *Applied Thermal Energy*, Elsevier Science, Vol. 23, pp. 1453-1487, ISSN 1359-4311.

Ferrari, M. L. (2011). Solid Oxide Fuel Cell Hybrid System: Control Strategy for Stand-Alone Configurations. *Journal of Power Sources*, Elsevier, Vol. 196, Issue 5, pp. 2682-2690, ISSN: 0378-7753.

Tucker, D., Liese, E., Gemmen, R. (2009). Determination of the Operating Envelope for a Direct Fired Fuel Cell Turbine Hybrid Using Hardware Based Simulation. *Proceedings of International Colloquium on Environmentally Preferred Advanced Power Generation 2009,* ICEPAG2009-1021, ISBN 3-7667-1662-X, Newport Beach, California, USA.

Hohloch, M., Widenhorn, A., Lebküchner, D., Panne, T., Aigner, M. (2008). Micro Gas Turbine Test Rig for Hybrid Power Plant Application. *Proceedings of ASME Turbo Expo 2008*, GT2008-50443, ISBN 0791838242, Berlin, Germany.

Ferrari, M. L., Pascenti, M., Bertone, R., Magistri, L. (2009a). Hybrid Simulation Facility Based on Commercial 100 kWe Micro Gas Turbine. *Journal of Fuel Cell Science and Technology*, Vol. 6, pp. 031008_1-8, ISSN: 1550-624X, New York, New York (USA).

Ferrari, M. L., Pascenti, M., Magistri, L., Massardo, A. F. (2010a). Hybrid System Test Rig: Start-up and Shutdown Physical Emulation, *Journal of Fuel Cell Science and Technology,* Vol. 7, pp. 021005_1-7, ISSN: 1550-624X, New York, New York (USA).

Ferrari, M. L., Pascenti, M., Magistri, L., Massardo, A. F. (2010b). Analysis of the Interaction Between Cathode and Anode Sides With a Hybrid System Emulator Test Rig, *Proceedings of International Colloquium on Environmentally Preferred Advanced Power Generation 2010,* ICEPAG2010-3435, Costa Mesa, CA (USA).

Turbec T100 Series 3 (2002). Installation Handbook.

Pascenti, M., Ferrari, M. L., Magistri, L., Massardo, A. F. (2007). Micro Gas Turbine Based Test Rig for Hybrid System Emulation, *Proceedings of ASME Turbo Expo 2007*, GT2007-27075, ISBN: 0791837963, Montreal, Canada.

Traverso, A. (2005). TRANSEO Code for the Dynamic Performance Simulation of Micro Gas Turbine Cycles, *Proceedings of ASME Turbo Expo 2005*, GT2005-68101, ISBN: 0791846997, Reno, Nevada (USA).

Traverso, A., Calzolari, F., Massardo, A. F. (2005). Transient Behavior of and Control System for Micro Gas Turbine Advanced Cycles, *Journal of Engineering for Gas Turbine and Power*, Vol. 127, pp. 340-347, ISSN: 0742-4795, New York, New York (USA).

Ferrari, M. L., Liese, E., Tucker, D., Lawson, L., Traverso, A., Massardo, A. F. (2007). Transient Modeling of the NETL Hybrid Fuel Cell/Gas Turbine Facility and Experimental Validation, *Journal of Engineering for Gas Turbines and Power*, Vol. 129, pp. 1012-1019, ISSN: 0742-4795, New York, New York (USA).

Caratozzolo, F., Traverso, A., Massardo, A. F. (2010).Development and Experimental Validation of a Modelling Tool for Humid Air Turbine Saturators, *Proceedings of ASME Turbo Expo 2010,* ASME Paper GT2010-23338, ISBN: 9780791838723, Glasgow, UK.

Bagnasco, M. (2011). Emulation of SOFC Hybrid System With Experimental Test Rig and Real-Time Model, Bachelor Thesis, TPG, Genova, Italy (in Italian).

Ferrari, M. L., Pascenti, M., Traverso, A. N., Massardo, A. F. (2011). Hybrid System Test Rig: Chemical Composition Emulation With Steam Injection, *Proceedings of International Conference on Applied Energy*, pp. 2821-2832, Perugia, Italy.

Ferrari, M. L., Bernardi, D., Massardo, A. F. (2006). Design and Testing of Ejectors for High Temperature Fuel Cell Hybrid Systems, *Journal of Fuel Cell Science and Technology*, Vol. 3, pp. 284-291, ISSN: 1550-624X, New York, New York (USA).

Massardo, A. F., Magistri, L. (2003). Internal Reforming Solid Oxide Fuel Cell Gas Turbine Combined Cycles (IRSOFC-GT) – Part II: Energy and Thermoeconomic Analyses, *Journal of Engineering for Gas Turbines and Power*, Vol. 125, pp. 67-74, ISSN: 0742-4795, New York, New York (USA).

Ferrari, M. L., Pascenti, M., Magistri, L., Massardo, A. F., (2009b). Hybrid System Emulator Enhancement: Anodic Circuit Design, *Proceedings of International Colloquium on Environmentally Preferred Advanced Power Generation 2009*, ICEPAG2009-1041, Newport Beach, California, USA.

Ghigliazza, F., Traverso, A., Pascenti, M., Massardo, A. F. (2009a). Micro Gas Turbine Real-Time Modeling: Test Rig Verification", *Proceedings of ASME Turbo Expo 2009*, GT2009-59124, Orlando, Florida (USA).

Ghigliazza, F., Traverso, A., Massardo, A. F., Wingate, J., Ferrari, M. L. (2009b). Generic Real-Time Modeling of Solid Oxide Fuel Cell Hybrid Systems, *Journal of Fuel Cell Science and Technology*, Vol. 6, pp. 021312_1-7, ISSN: 1550-624X, New York, New York (USA).

Ferrari, M. L., Pascenti, M., Magistri, L., Massardo, A. F. (2010c), Micro Gas Turbine Recuperator: Steady-State and Transient Experimental Investigation, *Journal of Engineering for Gas Turbines and Power*, Vol. 132, pp. 022301_1-8, ISSN: 0742-4795, New York, New York (USA).

Prando, A., Poloni, M. (2010). Absorber Tri-generative System Based on a 100 kWe Micro Gas Turbine: Study and Plant Development, Bachelor Thesis, TPG, Genova, Italy (in Italian).

Ferrari, M. L., Traverso, A., Magistri, L., Massardo, A. F. (2005). Influence of the Anodic Recirculation Transient Behaviour on the SOFC Hybrid System Performance, *Journal of Power Sources*, Elsevier, Vol. 149, pp. 22-32, ISSN: 0378-7753.

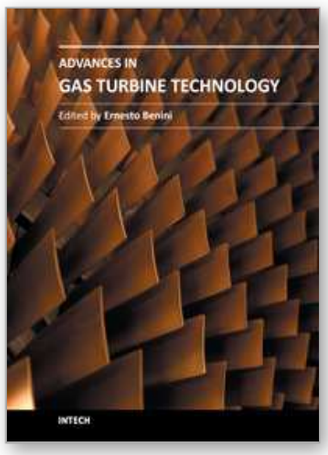

Advances in Gas Turbine Technology

Edited by Dr. Ernesto Benini

ISBN 978-953-307-611-9
Hard cover, 526 pages
Publisher InTech
Published online 04, November, 2011
Published in print edition November, 2011

Gas turbine engines will still represent a key technology in the next 20-year energy scenarios, either in stand-alone applications or in combination with other power generation equipment. This book intends in fact to provide an updated picture as well as a perspective vision of some of the major improvements that characterize the gas turbine technology in different applications, from marine and aircraft propulsion to industrial and stationary power generation. Therefore, the target audience for it involves design, analyst, materials and maintenance engineers. Also manufacturers, researchers and scientists will benefit from the timely and accurate information provided in this volume. The book is organized into five main sections including 21 chapters overall: (I) Aero and Marine Gas Turbines, (II) Gas Turbine Systems, (III) Heat Transfer, (IV) Combustion and (V) Materials and Fabrication.

INTECH
open science | open minds

InTech Europe
University Campus STeP Ri
Slavka Krautzeka 83/A
51000 Rijeka, Croatia
Phone: +385 (51) 770 447
Fax: +385 (51) 686 166
www.intechopen.com

InTech China
Unit 405, Office Block, Hotel Equatorial Shanghai
No.65, Yan An Road (West), Shanghai, 200040, China
中国上海市延安西路65号上海国际贵都大饭店办公楼405单元
Phone: +86-21-62489820
Fax: +86-21-62489821

IntechOpen